The Electronic Structure of Heteroannelated Cyclooctatetraenes and their UV–Vis Absorption Spectra

ARTICLE *in* CHEMISTRY OF HETEROCYCLIC COMPOUNDS · MAY 2014

Impact Factor: 0.62 · DOI: 10.1007/s10593-014-1482-7

CITATIONS
6

READS
25

3 AUTHORS:

Gleb Baryshnikov
KTH Royal Institute of Technology
74 PUBLICATIONS **503** CITATIONS
SEE PROFILE

Nataliya N. Karaush
Cherkasy State University, Bogdan Khmelni…
17 PUBLICATIONS **84** CITATIONS
SEE PROFILE

Boris Minaev
Черкаський національний університ…
327 PUBLICATIONS **3,188** CITATIONS
SEE PROFILE

Chemistry of Heterocyclic Compounds, Vol. 50, No. 3, June, 2014 (Russian Original Vol. 50, No. 3, March, 2014)

THE ELECTRONIC STRUCTURE OF HETEROANNELATED CYCLOOCTATETRAENES AND THEIR UV-VIS ABSORPTION SPECTRA

G. V. Baryshnikov[1], N. N. Karaush[1], and B. F. Minaev[1,2]*

The electronic structure and the UV-Vis absorption spectra of heteroannelated cyclooctatetraene derivatives are studied by density functional theory and by its non-stationary variant, the time-dependent density functional theory. The cyclooctatetraene ring is shown to be planar in all of the molecules considered, except the annelated fluorene and dibenzothiophene derivatives, and exhibits an antiaromatic character according to the magnetic and structural aromaticity criteria. The double ionization of annelated cyclooctatetraene molecules (quasi-circulenes) causes a change in the aromatic properties of cyclooctatetraene, which generally gaines aromaticity by double reduction and becomes non-aromatic upon double oxidation. The time-dependent density functional theory calculations enable the interpretation of electronic absorption spectra of recently synthesized quasi-circulenes and to predict the spectra of new, hypothetical molecules, which are important for the general theoretical understanding of hetero[8]circulene spectra.

Keywords: annelated cyclooctatetraenes, antiaromaticity, aromaticity, density functional theory, electronic absorption spectrum.

Partially annelated circulenes (quasi-circulenes) **1**-**9** (Fig. 1) are members of the planar (or quasi-planar) cyclooctatetraene (COT) family, and the molecules of some quasi-circulenes contain olefinic protons directly bound to the eight-membered ring [1-4], enabling the indirect study of their aromaticity by ^{1}H NMR spectroscopy. The first synthesized examples of quasi-circulenes were dehydrohelicenes [5-8], obtained by intramolecular cyclization of the respective heterohelicenes [7] and serving as the starting materials for the synthesis of thio[7]circulenes. Subsequently the dehydrohelicene **4** with an internal eight-membered framework was synthesized [9, 10], as well as the cyclic dimer of dithienothiophene [11]. The obtained compounds contained no olefinic protons, thus no data on the aromaticity of the internal eight-membered ring could be obtained from ^{1}H NMR spectra.

The number of quasi-circulenes containing such unsubstituted protons was limited until recently to just two hydrocarbons **8** [3] and **9** [1], in which COT was annelated with fluorene and biphenyl, respectively.

*To whom correspondence should be addressed, e-mail: glebchem@rambler.ru.

[1]Bogdan Khmelnitsky National University, 81 T. Shevchenko Blvd., Cherkasy 18031, Ukraine.
[2]Tomsk State University, 36 Lenina Ave., Tomsk 634050, Russia.

Translated from Khimiya Geterotsiklicheskikh Soedinenii, No. 3, pp. 381-396, 2014. Original article submitted January 27, 2014.

However, the synthesis of the first dithienothiophene-annelated COT **1** containing unsubstituted olefinic hydrogen atoms was reported by Aita et al. in 2013 [4]. The presence of these protons was manifested as ^{1}H NMR signals at 4.4-4.7 ppm, which provided evidence for the antiaromatic character of the internal eight-membered ring.

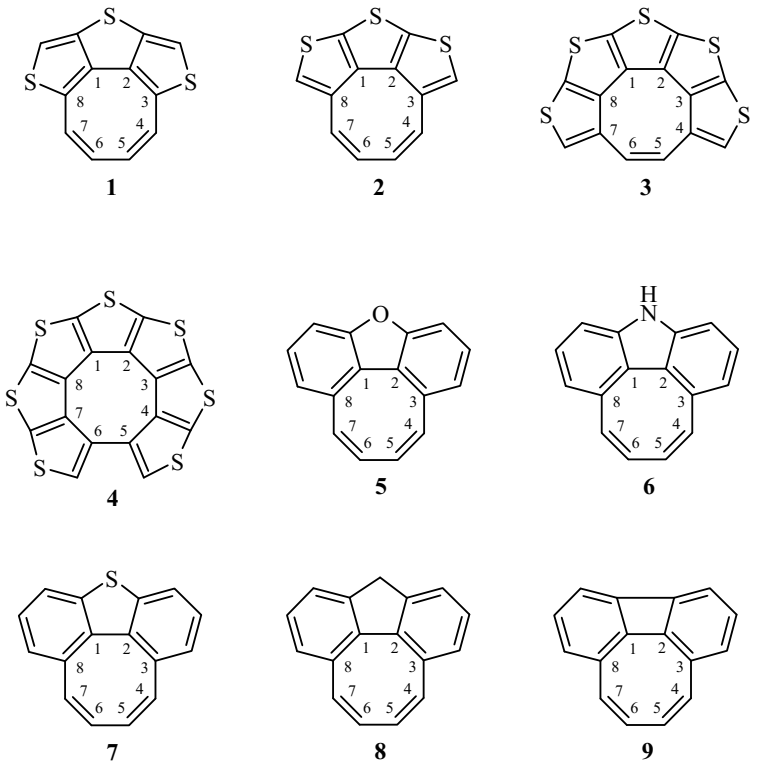

Fig. 1. The structural formulas of the partially annelated circulenes **1**-**9** and the atom numbering in the cyclooctatetraene ring.

In view of the recent results, computational methods of quantum chemistry should be employed for the prediction of new heterocyclic quasi-circulenes and the investigation of electronic structure, aromaticity, and absorption spectra of these molecules. The current work presents quantum chemistry modeling results and the associated properties of several synthesized quasi-circulenes **1**, **4**, **8**, **9** (Fig. 1), as well as predicts some new quasi-circulenes **2**, **3**, **5**-**7**. The aromaticity of all the examined compounds was compared in neutral and doubly ionized forms, and the UV-Vis electronic spectra were analyzed. The interest in eight-membered carbocyclic compounds has increased in recent years [4, 7, 10, 11] after the discovery of sulflowers [9] and new synthetic approaches to heterocirculenes. Partially annelated circulenes and their ions are important for a deeper understanding of aromaticity in the COT family of compounds [4]. The investigated quasi-circulenes are of practical interest as promising organic semiconductors, and also as starting compounds for the synthesis of new circulenes and related materials.

Computational approaches. The equilibrium structures of neutral quasi-circulenes **1**-**9**, their dications and dianions in singlet and triplet states were optimized by density functional theory (DFT) calculations using the B3LYP hybrid functional [12, 13] in 6-31G(d,p) basis set [14], which contained polarization functions (the triplet states were calculated by the spin unrestricted UB3LYP method). The split-valence double basis set 6-31G(d,p) was selected for the optimization procedure due to the combination of a good accuracy and acceptable duration of computation. For instance, the expansion of basis set by increasing the multiple splitting of the valence shell and adding diffuse functions led to a substantial increase of computational time, while the structural parameters of the

investigated systems were not significantly refined (the changes in bond lengths did not exceed 0.002 Å, while the valence angles changed by no more than 0.25°).

In the current work we also calculated the normal vibration frequencies for the investigated neutral molecules and the corresponding ions. The normal vibration frequencies were real numbers in all cases, proving that a true minimum on the full energy hypersurface (excluding the kinetic energy of the nuclei) was found for the particular molecule.

The obtained optimized geometry of the singlet ground state of the neutral molecules **1**-**9** was also used for the calculation of vertical electronic transition spectra within the framework of time-dependent density functional theory (TD DFT) in the vacuum approximation and by using the polarizable continuum model of solvation PCM [15] (solvent – dichloromethane), which was used for the experimental investigation of absorption spectra [4]. The calculated electronic absorption spectra of the molecules **1**-**9** were created by using the SWizard software [16] (band half-width 3000 cm^{-1}, Gaussian distribution).

The aromatic properties of the quasi-circulenes **1**-**9** and the corresponding dications and dianions in the electronic ground state were studied within the framework of nucleus-independent chemical shift (NICS) theory [17, 18]. The tensors of nuclear magnetic shielding for each atom, including the point of "imaginary atoms" (Bq), were calculated through the approximation of calibration-invariant atomic orbitals (GIAO) [19] with the B3LYP/6-311++G(d,p) [20, 21] method (using the 6-311++G(d,p) basis set for the calculation of NICS indexes recommended in the work [17]). The positions of the Bq atoms were determined by finding the coordinates of the (3, +1) critical points in the cycle according to the QTAIM method [22] by using the AIMAII program [23] (the NICS(0) indexes corresponded to these points; the NICS(1) indexes corresponded to the points 1 Å above the center). The values of NICS(1) indexes are commonly used to better account for the magnetic π-electron effects, compared to the NICS(0) indexes [17]. Negative values of the NICS(0) and NICS(1) indexes indicate the existence of induced diatropic ring currents, i.e., aromaticity; positive values of the NICS(0) and NICS(1) indexes correspond to paratropic ring currents, i.e., antiaromaticity [17]. In the cases when the absolute values of NICS(0) and NICS(1) are close to zero, the ring is non-aromatic. All DFT calculations were performed with the Gaussian 09 software suite [24] on PDC supercomputer at the Royal Institute of Technology, Stockholm, Sweden.

Molecular geometry and aromatic properties. The calculation of the equilibrium geometry parameters showed that the investigated molecules are planar and correspond to the C_{2v} point group of symmetry. The molecules of compounds **7** and **8** were exceptions, characterized by a slight out-of-plane deformation and corresponding to the C_2 point group of symmetry. An important parameter of the investigated molecules was the alternating bond length (ΔR) in the COT ring (Table 1), calculated as the mean difference in bond lengths, which can be described by the formula:

$$\Delta R = \frac{\sum_{i=1}^{8} \left| a_i - a_i^* \right|}{8},$$

where a and a^* – the lengths of two adjacent C–C bonds (a total of 8 pairs in COT). The ΔR parameter can be interpreted as a structural criterion of aromaticity: the cases of pronounced alternation of single and double bonds within a ring are associated with high ΔR values and point to an antiaromatic character of the ring (for example, for a hypothetical planar COT of D_{4h} symmetry ΔR = 0.121 Å [25], for cyclobutadiene ΔR = 0.227 Å [26]), while ΔR values close to zero (or equal to zero, as in benzene molecule) indicate cyclic conjugation associated with aromatic properties and stabilization of such a ring system.

As evidenced by this criterion, the COT ring in the molecules of the quasi-circulenes **1**-**9** provides antiaromatic or weakly antiaromatic character (the corresponding ΔR values varied from 0.11 Å for the circulene **9** to 0.02 Å for the dehydrohelicene **4**). Quantum-chemical calculations of the NICS(0) and NICS(1) indexes by the GIAO/B3LYP/6-311++G(d,p) method confirmed the conclusion regarding the antiaromaticity of the internal eight-membered ring of the quasi-circulenes **1**-**9**, based on the positive values of NICS(0) and NICS(1) (Figs. 2 and 3).

We observed that the aromaticity of the dithienothiophene quasi-circulenes **1** and **2** strongly depended on the sulfur atom position in the annelating fragment. For example, the COT ring of the quasi-circulene **1** is strongly antiaromatic (NICS(0) = +22.7, NICS(1) = +17.5 ppm, ΔR = 0.091 Å) and has similar properties to the free (not annelated) COT of D_{4h} symmetry (NICS(0) = +41.7 ppm, ΔR = 0.121 Å). For the hypothetical quasi-circulene **2** the analogous values of NICS(0), NICS(1), and ΔR were much lower and equal to just +6.2 ppm, +3.5 ppm, and 0.053 Å, respectively, which indicates a weak antiaromatic character of the COT (Fig. 2). Such a pronounced difference between the NICS and ΔR indexes of the two isomers **1** and **2** is explained by the disrupted sequence of C–C bonds in the COT ring of the quasi-circulene **2**. The calculated lengths of the C(1)–C(8), C(1)–C(2), and C(2)–C(3) bonds of the COT ring shared with the three thiophene rings of compound **2** (Fig. 1) were nearly identical, with a variation of merely 0.01 Å (Table 1), thus disrupting the antiaromaticity criterion of the COT ring, which requires a clear alternation of single and double bonds.

TABLE 1. The Geometry Parameters of Eight-membered Rings of Neutral Molecules of Compounds **1-9** (Emphasized in Bold) and the Corresponding Dications and Dianions*

Com-pound	M	ω_1, cm^{-1}	Bond length, Å					ΔR, Å
			C(1)–C(2)	C(2)–C(3) C(1)–C(8)	C(3)–C(4) C(8)–C(7)	C(4)–C(5) C(7)–C(6)	C(5)–C(6)	
1	1	55.9	**1.458**	**1.379**	**1.455**	**1.355**	**1.464**	**0.091**
1^{2+}	1	56.6	1.400	1.450	1.374	1.439	1.379	0.063
1^{2-}	1	64.0	1.436	1.427	1.399	1.420	1.402	0.034
2	1	70.8	**1.433**	**1.445**	**1.452**	**1.358**	**1.455**	**0.053**
2^{2+}	1	59.3	1.415	1.463	1.381	1.446	1.377	0.066
2^{2-}	1	64.2	1.465	1.476	1.403	1.433	1.385	0.041
3	1	57.8	**1.422**	**1.428**	**1.444**	**1.462**	**1.359**	**0.036**
3^{2+}	3	62.5	1.382	1.423 1.445	1.443 1.462	1.428 1.388	1.402	0.034
3^{2-}	1	61.1	1.443	1.444	1.466	1.408	1.437	0.028
4	1	6.0	**1.416**	**1.423**	**1.442**	**1.459**	**1.496**	**0.020**
4^{2+}	3	41.4	1.417	1.393	1.434	1.451	1.466	0.055
4^{2-}	1	39.7	1.455	1.499 1.445	1.465 1.441	1.469 1.449	1.479	0.023
5	1	32.2	**1.470**	**1.420**	**1.465**	**1.352**	**1.454**	**0.078**
5^{2+}	1	38.8	1.416	1.467	1.395	1.428	1.381	0.051
5^{2-}	1	81.1	1.444	1.467	1.410	1.414	1.398	0.025
6	1	13.9	**1.472**	**1.424**	**1.466**	**1.351**	**1.451**	**0.076**
6^{2+}	1	19.6	1.410	1.474	1.394	1.427	1.378	0.057
6^{2-}	1	75.3	1.452	1.470	1.412	1.413	1.397	0.023
7	1	74.5	**1.476**	**1.425**	**1.480**	**1.341**	**1.455**	**0.090**
7^{2+}	1	59.7	1.426	1.477	1.391	1.432	1.366	0.061
7^{2-}	1	41.7	1.462	1.491	1.415	1.407	1.392	0.032
8	1	59.3	**1.495**	**1.417**	**1.475**	**1.345**	**1.455**	**0.094**
8^{2+}	1	41.1	1.449	1.471	1.397	1.424	1.375	0.043
8^{2-}	1	52.6	1.471	1.476	1.415	1.410	1.395	0.022
9	1	69.5	**1.484**	**1.370**	**1.466**	**1.358**	**1.480**	**0.110**
9^{2+}	1	86.5	1.406	1.424	1.421	1.402	1.427	0.016
9^{2-}	1	103.2	1.446	1.419	1.411	1.426	1.418	0.015

*M – the spin multiplicity of the ground state: M = 2S + 1, where S – total spin quantum number; ω_1 – frequency of the first vibrational mode, ΔR – bond length alternation parameter.

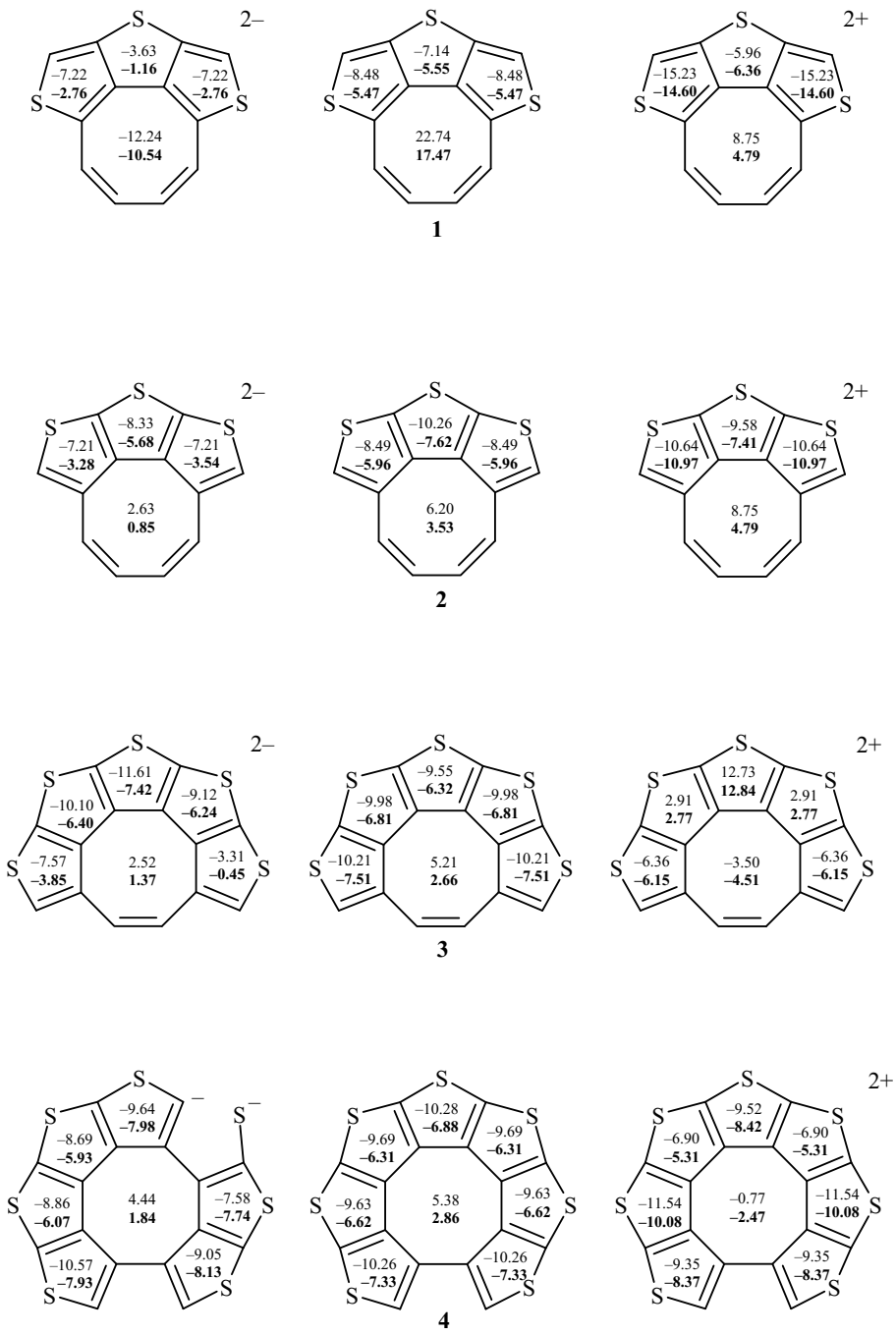

Fig. 2. The values of NICS(0) (top) and NICS(1) (bottom) indexes in neutral molecules, dianions, and dications of the quasi-circulenes **1**-**4**.

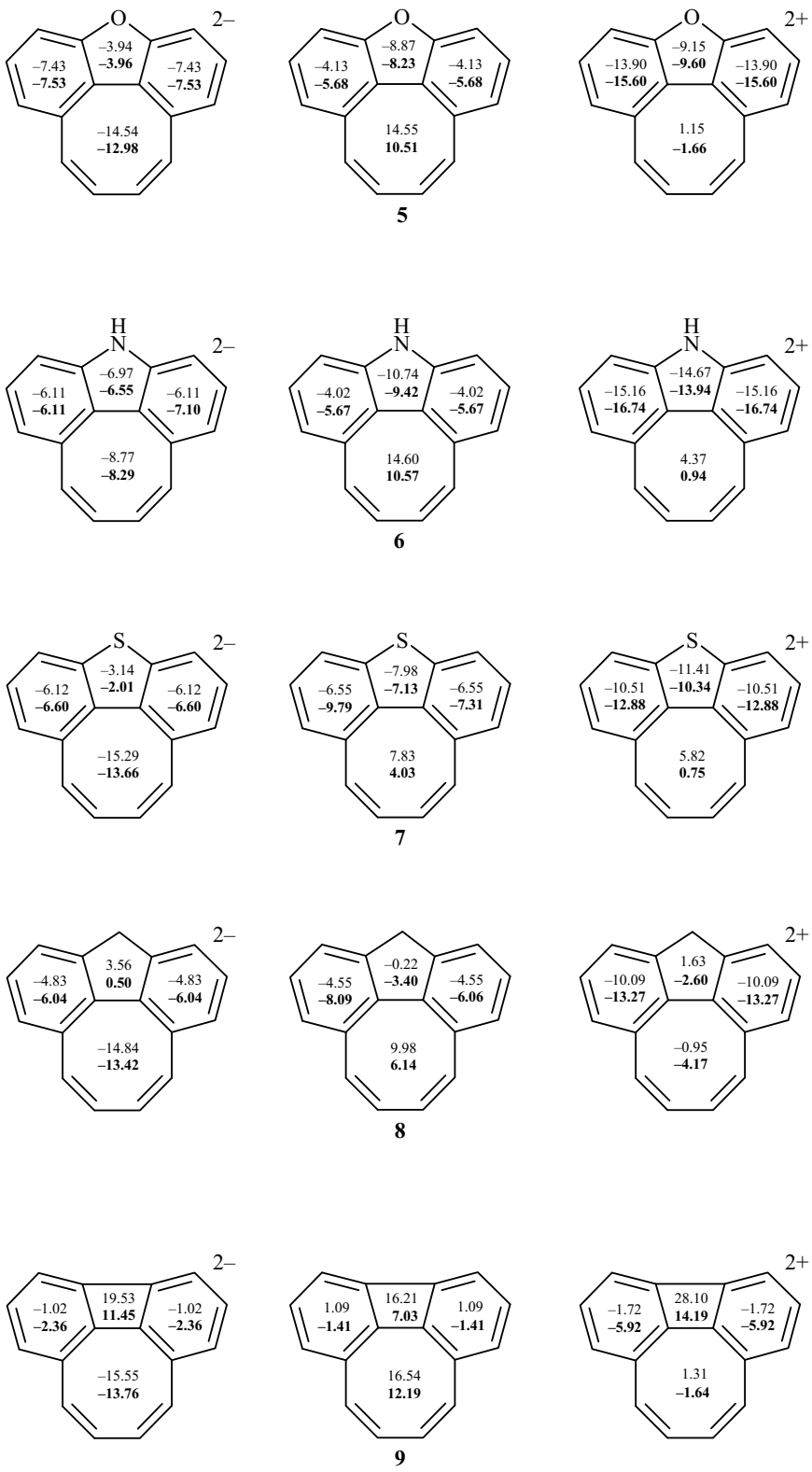

Fig. 3. The values of the NICS(0) (top) and NICS(1) (bottom) indexes in neutral molecules, dianions, and dications of the quasi-circulenes **5-9**.

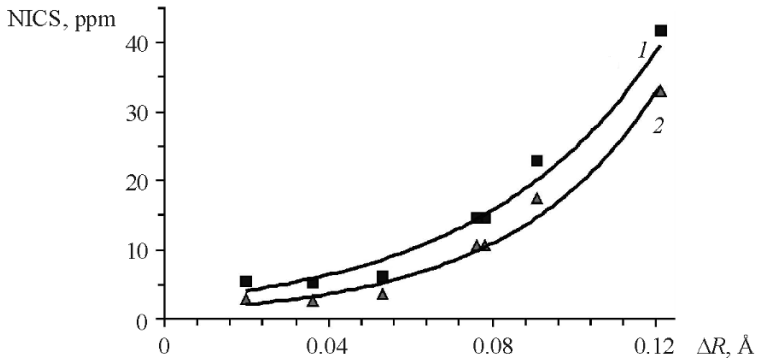

Fig. 4. The dependence of bond length alternation parameter (ΔR) on the values of NICS(0) (curve *1*) and NICS(1) (curve *2*) indexes for the COT ring in the molecules **1**-**6**, as well as in the non-annelated cyclooctatetraene of D_{4h} symmetry.

Figure 4 shows the correlation between the alternation parameter (ΔR) of COT and the values of NICS(0) and NICS(1) indexes in the molecules of compounds **1**-**6** (the dataset also includes the parameters of hypothetical non-annelated cyclooctatetraene of D_{4h} symmetry). A least squares approximation showed that the correlation was best described by exponential curves of the type NICS(0) = $2.584e^{22.57\Delta R}$ and NICS(1) = $1.192e^{27.63\Delta R}$ (the correlation coefficient $R^2 = 0.95$). This correlation did not apply to the molecules of quasi-circulenes **7** and **8** due to their nonplanar structures, and also to the molecule of quasi-circulene **9**, which featured a unique system of two adjacent antiaromatic four- and eight-membered rings (Fig. 4).

The strictly alternating sequence of single and double bonds in the hypothetical quasi-circulenes **2**-**4** with an odd number of thiophene fragments did not allow us to predict the existence of analogous quasi-circulenes with even numbers of thiophene rings. These compounds would have to contain at least one sp^3-hybridized carbon atom in the annelating nucleus or have a cationic structure (as shown in Fig. 5*a*,*c*,*d*), in order to meet the criteria for a planar COT.

Double ionization of the quasi-circulenes **1**, **5**-**9** produces species analogous to tetraoxo[8]circulenes and azaoxo[8]circulenes [27-30], while the COT ring gains an aromatic character in the dianions of the quasi-circulenes **1**, **5**-**9**. The dianions of the hypothetical quasi-circulenes **2**-**4** have a weakly aromatic (nearly non-aromatic) internal eight-membered ring, as evidenced by the small positive values of NICS(0) and NICS(1). A double oxidation of the quasi-circulenes **7**-**9** leads to out-of-plane deformation of the COT ring, which, however, acquires a non-aromatic character in the entire series of the dications **5**-**9**. The annelating fragments in this situation are still characterized by diatropic ring currents.

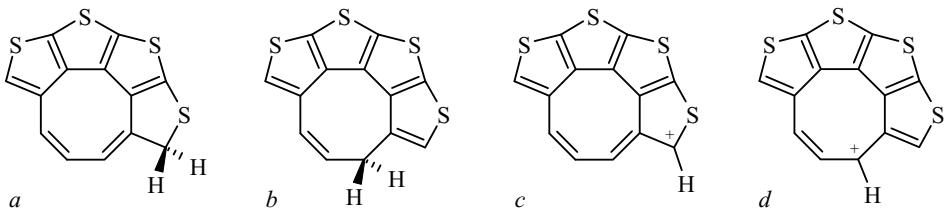

Fig. 5. Theoretical neutral (*a*,*b*) and cationic (*c*,*d*) structures of quasi-circulenes with an even number of thiophene rings (examples with four thiophene rings are shown).

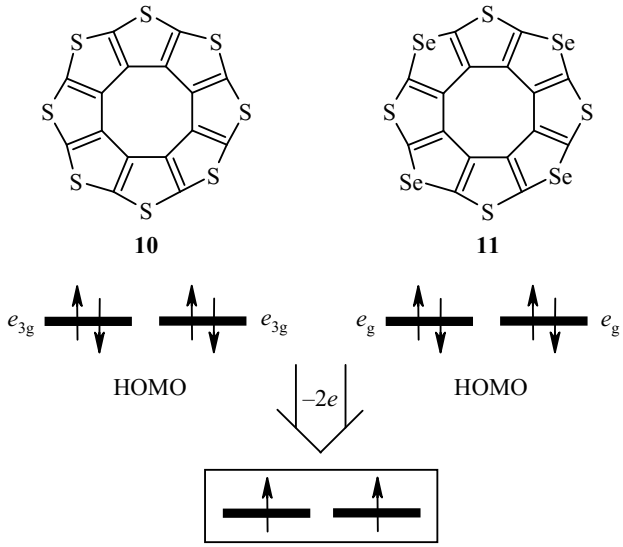

Fig. 6. The effects of double oxidation on the molecules of thio[8]circulenes **10** and **11**.

The dications of compounds **1** and **2** have a planar structure, while the COT ring remains antiaromatic, similarly to the neutral molecule (Fig. 3). Remarkably, our calculations predicted a triplet ground state for the dications of the quasi-circulenes **3** and **4**, which is also characteristic of the octathio[8]circulene **10** [31] and the *sym*-tetrathiotetraseleno[8]circulene **11** [32] (Fig. 6). Calculations according to the DFT/B3LYP/6-31+G(d) method indicated that the highest occupied molecular orbital (HOMO) in the molecules **10** and **11** is doubly degenerate (Fig. 6). Subsequently, double ionization (oxidation) of the circulenes **10** and **11** according to the classical Hund rules must lead to the formation of dications in triplet state. This assumption was first formulated [33] for the sulflower **10** without any experimental or theoretical proof. Our DFT/B3LYP/ 6-31G(d,p) calculations prove that triplet state is the ground state for the dications of the sulflowers **10** and **11**, where the thiophene and selenophene rings in these triplet species are aromatic (NICS(0) and NICS(1) < 0), but the COT ring is non-aromatic (the NICS(0) and NICS(1) indexes are close to zero).

The singlet state of the dications of compounds **10** and **11** is 4 kcal/mol higher in energy, compared to the triplet ground state. In addition, the dications in singlet state are fully antiaromatic (i.e., destabilized), including the thiophene and selenophene rings.

Analysis of the electronic absorption spectra. The UV-Vis absorption spectrum of compound **1** in dichloromethane solution (Fig. 7) was first recorded and published in the work [4]. We interpreted the observed spectrum of the molecule **1**, which belongs to the C_{2v} point group of symmetry, by calculating the energy of 25 vertical singlet-singlet electronic transitions using the TD DFT method. The experimental spectrum contained a very weak absorbtion in the region of 750-450 nm (inset in Fig. 7, curve *3*). Our calculations predict only a single transition in this region at 721 nm, with $X^1A_1 \rightarrow 1^1B_2$ symmetry (the configuration of HOMO → LUMO gives the dominant contribution to the electronic state 1^1B_2, Table 2, Fig. 7). We interpreted all other experimentally observed absorption bands in the region of 700-450 nm as vibronic progression of the first band at 722 nm. Remarkably, the 0–0 transition at 722 nm was of lower intensity than the 0–1 transition at 657 nm (Fig. 7), which indicated a major change of molecular geometry upon electronic transition and a low value of Franck–Condon factor for the 0–0 overlap of vibrational functions [34].

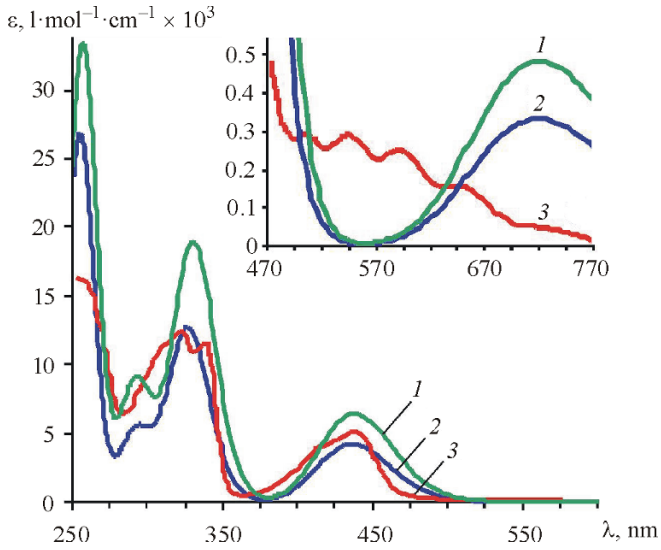

Fig. 7. The UV-Vis absorption spectrum of compound **1**: *1* – calculated by taking into account the solvent effect of CH_2Cl_2, *2* – calculated in vacuum approximation, *3* – experimental absorption spectrum (recorded in CH_2Cl_2).

A more intense absorption band was observed in the region of 450-400 nm, with a maximum at 440 nm, and was interpreted as corresponding to the electronic transition of $X^1A_1 \rightarrow 1^1A_1$ symmetry into the S_2 excited state at 438 nm (Table 2, Fig. 7).

The experimentally observed absorption for compound **1** in the region of 350-300 nm (a doublet band with maxima at 324 and 339 nm, Fig. 7) [4] matched the calculated band at 331 nm (Table 2) due to the highly allowed $X^1A_1 \rightarrow 2^1B_2$ transition into the excited state S_3. It was assumed that the second observed maximum in this region at 324 nm, which had no counterpart in the calculated spectrum, was a vibronic satellite of the band at 339 nm, induced by stretching vibrations of ν(CC) ~1360 cm^{-1}.

The experimentally obtained absorption spectrum of compound **1** also contained a weak absorption in the region of 300-280 nm (manifested as a shoulder on the left side of the band at 318 nm) [4], which we assigned to the calculated vertical electronic transition $X^1A_1 \rightarrow 2^1A_1$ with a maximum at 293 nm (Table 2, Fig. 7). Our calculations also provided a good match for the observed UV band at 260 nm.

TABLE 2. The Experimentally Observed and Theoretically Calculated (TD DFT Method) Wavelengths (λ) and Intensities (ε) of Electronic Absorption Spectra for Compound **1**

$\lambda_{calc}/\lambda_{obs}$, nm*	ε_{calc} / ε_{obs}, $l \cdot mol^{-1} \cdot cm^{-1} \times 10^4$	Assignment	*f*
721/722	0.05/0.005	S_1: $X^1A_1 \rightarrow 1^1B_2$	0.007
438/440	0.64/0.50	S_2: $X^1A_1 \rightarrow 1^1A_1$	0.089
331/324(339)	1.90/1.27(1.15)	S_3: $X^1A_1 \rightarrow 2^1B_2$	0.261
293/289	0.92/0.89	S_5: $X^1A_1 \rightarrow 2^1A_1$	0.124
259/260	3.33/1.61	S_9: $X^1A_1 \rightarrow 3^1A_1$	0.312

*The calculated absorbtion maxima λ_{calc} correspond to vertical electronic transitions, according to our interpretation (the number of electronic state and symmetry of transition), and the oscillator strength (*f*).

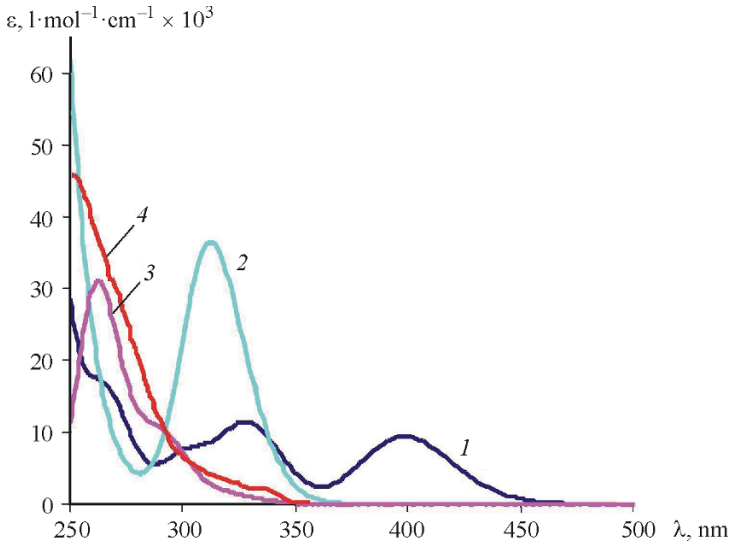

Fig. 8. The UV-Vis absorption spectra of: *1* – compound **2**, *2* – compound **3**, *3* – compound **4**; *4* – the experimentally recorded spectrum of compound **4** [10] (calculations performed by taking into account the solvent effects of CH_2Cl_2 according to the PCM model).

The UV-Vis absorption spectra of other sulfur-containing heteroannelated cyclooctatetraenes **2**-**4** with a variable number of thiophene rings are presented in Fig. 8. As shown in the Figures 7 and 8, a characteristic spectral feature of the isomeric quasi-circulenes **1** and **2** is the absence of any absorption around 720 nm for compound **2**, the calculated spectrum of which contains the first band (the $S_0 \rightarrow S_1$ transition) at 398 nm (Fig. 8). This fact was adequately explained by the molecular orbital diagram (Fig. 9). The HOMO → LUMO configuration provided the dominant contribution to the $S_0 \rightarrow S_1$ transition for both isomers. However, in the case of the isomeric quasi-circulene **2**, the gap between the frontier orbitals was significantly increased compared to compound **1**, due to the different position of sulfur atoms in the annelating fragment (Fig. 9) and redistribution of the frontier orbital wave functions, which caused the S_1 state of compound **2** to have a higher energy.

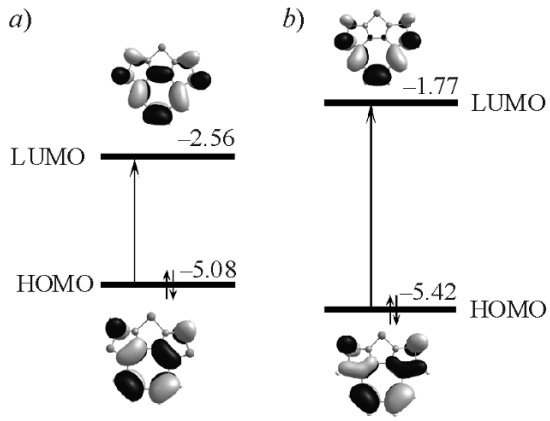

Fig. 9. A diagram of molecular orbitals illustrating the first electronic transition in the molecules **1** (*a*) and **2** (*b*).

As shown in Figure 8, TD DFT calculations provided a good match for the experimentally observed spectrum of compound **4** [10] (curves *3* and *4*). For example, the weak absorption in the 340-300 nm region of the experimental spectrum, manifested as a broadening on the right side of the 252 nm band, corresponds to the weakly allowed transitions into the S_1, S_2, and S_3 states at 320 ($f = 0.017$), 313 ($f = 0.001$), and 301 nm

(f = 0.0004), respectively (Fig. 8). The intense absorption in the region of 300-280 nm (curve *4*) was caused mainly by the transition to the S_5 state at 292 nm (a shoulder on the right side, curve *3*). The experimental spectrum in the region of 280-250 nm had an intense absorption band with a maximum at 252 nm, which we assigned to the calculated band with absorption maximum at 262 nm.

The spectrum of compound **3** was different from those of the quasi-circulenes **2** and **4** by the presence of an intense absorption band with maximum at 311 nm, caused by electronic transition to the S_3 excited state, the nature of which can be interpreted as a mixture of three configurations, HOMO → LUMO, HOMO-2 → LUMO, HOMO-2 → LUMO+2. The nearby transitions $S_0 \rightarrow S_1$ and $S_1 \rightarrow S_2$ were also calculated to occur in this region (326 and 323 nm), and had a relatively low intensity ($f \approx 0.1$), manifested in the UV spectrum as a broadening on the right side of the band (Fig. 8).

This work predicts for the first time the absorption spectra of the hypothetical quasi-circulenes **5**-**7**, which are heterocyclic analogs of the well-known hydrocarbon **8**. Figure 10 demonstrates that the spectra of these compounds are quite similar. For instance, there is a good match of the weak absorption in the long-wavelength region in the spectra of compounds **5** and **6** with a maximum at 540 nm (Table 3, inset in Fig. 10), which we assigned to the $X^1A_1 \rightarrow {}^1B_2$ transition (molecular symmetry C_{2v}). The molecule of quasi-circulene **7** is nonplanar and belongs to the C_2 point group of symmetry. Consequently, the first excited state of ^1B symmetry has a significantly higher energy and causes a very weak absorption in the spectra of the molecule **7** at 410 nm (Table 3), not readily apparent in Figure 10. According to our calculations, among compounds **5**-**7** only the quasi-circulene **6** shows visible light absorption (band maximum at 403 nm), which we assign to the weakly allowed transition of $X^1A_1 \rightarrow 1^1A_1$ symmetry (Table 3). The UV absorption spectra of all three compounds **5**-**7** were very similar, in particular the band with maximum at ~350 nm showed a good match (Table 3), and there was an increasing absorption in the region of 300-250 nm.

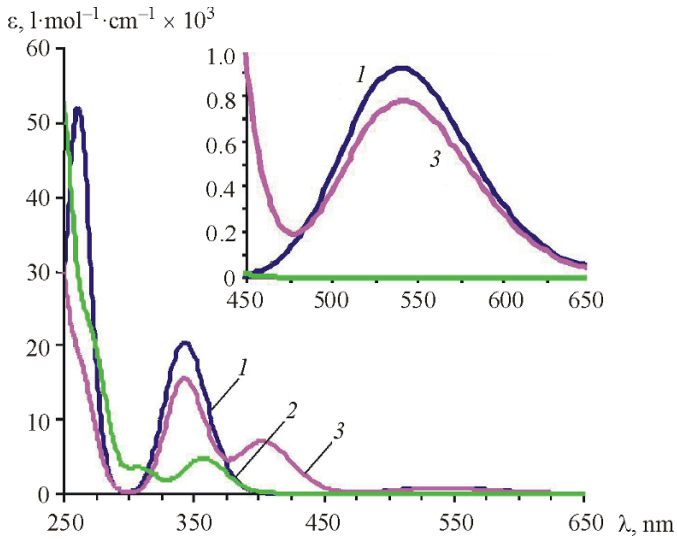

Fig. 10. The calculated UV-Vis absorption spectra of: *1* – compound **5**, *2* – compound **7**, *3* – compound **6** (the solvent effects of CH_2Cl_2 were taken into account, calculations performed with the PCM model).

The electronic absorption spectra of the hydrocarbon quasi-circulenes **8** and **9** were first discussed in the original publications [1, 3, 35] that described the synthesis and physicochemical properties of these compounds. The experimental data [3] about the absorption of the quasi-circulene **8** are limited to merely identification of one of the absorption maxima at 346 nm (Table 4), which we assigned to the weakly allowed transition to the electronic state 2^1B (the molecule has a C_2 symmetry). Additionally, in the spectrum of compound **8**

TABLE 3. The Absorption Maxima (λ), Intensities (ε), and Oscillator Strength (*f*) in the Electronic Absorption Spectra of Compounds **5**-**7** Calculated According to the TD DFT Method

λ_{calc}, nm	ε_{calc}, $l \cdot mol^{-1} \cdot cm^{-1} \times 10^4$	Assignment	*f*
Compound **5**			
540	0.09	S_1: $X^1A_1 \rightarrow 1^1B_2$	0.013
342	2.05	S_2: $X^1A_1 \rightarrow 1^1A_1$	0.103
		S_3: $X^1A_1 \rightarrow 2^1B_2$	0.202
262	5.21	S_4: $X^1A_1 \rightarrow 3^1B_2$	0.395
		S_5: $X^1A_1 \rightarrow 2^1A_1$	0.272
Compound **6**			
541	0.08	S_1: $X^1A_1 \rightarrow 1^1B_2$	0.011
403	0.70	S_2: $X^1A_1 \rightarrow 1^1A_1$	0.097
343	1.56	S_3: $X^1A_1 \rightarrow 2^1B_2$	0.215
268	1.40	S_4: $X^1A_1 \rightarrow 2^1A_1$	0.132
252	2.65	S_6: $X^1A_1 \rightarrow 3^1A_1$	0.178
Compound **7**			
410	0.02	S_1: $X^1A \rightarrow 1^1B$	0.001
357	0.48	S_2: $X^1A \rightarrow 1^1A$	0.067
309	0.36	S_3: $X^1A \rightarrow 2^1B$	0.048
250	5.29	S_6: $X^1A \rightarrow 4^1A$	0.138
		S_7: $X^1A \rightarrow 4^1B$	0.616

we predicted a very weak absorption at 455 nm, belonging to the first singlet–singlet transition of $X^1A \rightarrow 1^1B$ symmetry, and a high intensity absorption band with the maximum at 283 nm, that we assigned to the excitation of the molecule **8** into the state 3^1B (Fig. 11, Table 4).

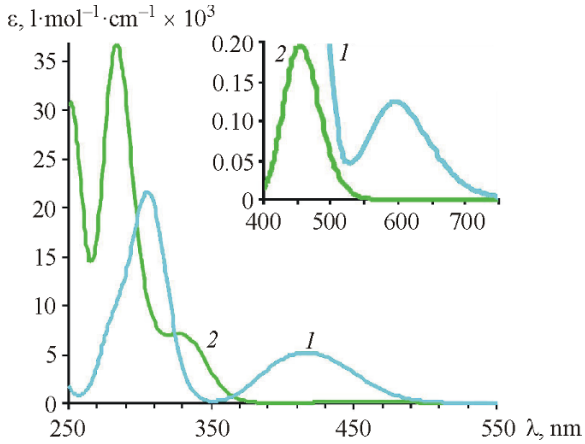

Fig. 11. The calculated UV-Vis absorption spectra of: *1* – compound **9**, *2* – compound **8** (calculated by taking into account the effect of the solvent (CH_2Cl_2) within the framework of the PCM model).

The absorption spectrum of compound **9** has been experimentally studied in detail [1, 35]. For instance, three main systems of bands have been identified in the spectrum of compound **9** [35]: the first one is a weak absorption band at 621 nm and its vibrational progression, including the maximum at 327 nm, an intense band at 305 nm with a vibrational structure to 258 nm, and an intense band at 225 nm ($\varepsilon_{exp} = 22.4 \cdot 10^4$ $l \cdot mol^{-1} \cdot cm^{-1}$).

TABLE 4. The Absorption Maxima (λ), Intensities (ε), and Oscillator Strength (*f*) in the Electronic Absorption Spectra of Compounds **8** and **9** Obtained Experimentally and Calculated According to the TD DFT Method

$\lambda_{calc}/\lambda_{exp}$, nm	$\varepsilon_{calc}/\varepsilon_{exp}$, $l \cdot mol^{-1} \cdot cm^{-1} \times 10^4$	Assignment	*f*
Compound **8**			
455	0.02	S_1: $X^1A \rightarrow 1^1B$	0.003
333/346	0.70/0.136	S_2: $X^1A \rightarrow 2^1B$	0.087
283	3.67	S_4: $X^1A \rightarrow 3^1B$	0.497
Compound **9**			
597/621	0.012/0.005	S_1: $X^1A_1 \rightarrow 1^1B_2$	0.002
416/(478–402)*	0.51/0.11	S_2: $X^1A_1 \rightarrow 2^1B_2$	0.051
		S_3: $X^1A_1 \rightarrow 3^1B_2$	0.045
306/305	2.16/2.04	S_4: $X^1A_1 \rightarrow 4^1B_2$	0.289

*The electronic and vibrational bands in the range of 478-402 nm in the experimentally obtained spectrum could not be completely resolved [35].

Our calculations adequately reproduced the first absorption band at 597 nm due to the electron transition of $X^1A_1 \rightarrow 1^1B_2$ symmetry (Table 4). Besides that, we predicted two closely spaced electronic transitions at 432 and 398 nm in the spectrum of compound **9**, corresponding to the calculated absorption band with a maximum at 416 nm (Fig. 11). Apparently, these electronic transitions were previously incorrectly assigned [35] to the vibrational progression of the first absorption band at 621 nm.

It should be pointed out that vibrational progression over such a wide range (621-327 nm) must be associated with a severe molecular geometry deformation of compound **9** in the excited state. However, geometry optimization of the first excited state S_1 showed that the molecule of compound **9** remained planar, with only the bond lengths in the COT ring becoming more equal, which was also characteristic of the T_1 electronic state. Thus, the minor molecular geometry deformation of compound **9** upon excitation to the first singlet state should not cause such a long vibronic progression over the broad range of 621-327 nm. The vibrational structure of the first band (621 nm) is most likely expressed over the much shorter spectral range of 621-512 nm, while the absorption bands at 478-402 nm are caused by two closely spaced transitions to the S_2 and S_3 states with the corresponding electronic-vibrational transitions.

In conclusion, we should note that the application of modern quantum chemistry methods to such highly symmetrical cyclic compounds as circulenes and quasi-circulenes is a promising approach for elaborating the concept of aromaticity [36-38]. In particular, we have shown that the COT ring of our investigated quasi-circulenes was in all cases characterized by the presence of antiaromatic paratropic (counterclockwise) ring currents, while the annelating part, to the contrary, had aromatic character due to diatropic (clockwise) ring current. As a result, quasi-circulenes may be considered to be nonaromatic, with compensated diatropic and paratropic ring currents, similarly to fullerene C_{60}, cycloparaphenylenes, and some other peculiar cyclic compounds [39]. This conclusion calls for an additional detailed analysis of magnetically induced ring currents [39-42], which will be the topic of our future research.

The analysis of excited states of symmetric molecules, including the considered quasi-circulenes, presents also fundamental interest for the general understanding of the spectra of these compounds. Our study represents the first effort at TD DFT calculation and analysis of quasi-circulenes. We have shown that the excited state energy levels of these compounds strongly depend on the position and type of heteroatoms in the annelating part of the molecules. In addition, the calculations performed for the synthesized circulenes allow a reliable assignment of the experimentally observed absorption bands to particular electronic transitions and also provide an opportunity for the first time to predict the spectra of some hypothetical quasi-circulenes, which may

be synthesized in the future. The vibrational spectra and semiconductor properties of quasi-circulenes are still not completely understood, and will be the subject of our future research.

REFERENCES

1. C. F. Wilcox, Jr., J. P. Uetrecht, and K. K. Grohman, *J. Am. Chem. Soc.*, **94**, 2532 (1972).
2. C. F. Wilcox, *J. Mol. Struct.: THEOCHEM*, **759**, 125 (2006).
3. I. Willner and M. Rabinovitz, *J. Org. Chem.*, **45**, 1628 (1980).
4. K. Aita, T. Ohmae, M. Takase, K. Nomura, H. Kimura, and T. Nishinaga, *Org. Lett.*, **15**, 3522 (2013).
5. M. B. Groen, H. Schadenberg, and H. Wynberg, *J. Org. Chem.*, **36**, 2797 (1971).
6. J. H. Dopper, D. Oudman, and H. Wynberg, *J. Am. Chem. Soc.*, **95**, 3692 (1973).
7. Y. Shen and C.-F. Chen, *Chem. Rev.*, **112**, 1463 (2012).
8. J. H. Dopper, D. Oudman, and H. Wynberg, *J. Org. Chem.*, **40**, 3398 (1975).
9. K. Yu. Chernichenko, E. S. Balenkova, and V. G. Nenajdenko, *Mendeleev Commun.*, **18**, 171 (2008).
10. A. Rajca, M. Miyasaka, S. Xiao, P. J. Boratynski, M. Pink, and S. Rajca, *J. Org. Chem.*, **74**, 9105 (2009).
11. T. Ohmae, T. Nishinaga, M. Wu, and M. Iyoda, *J. Am. Chem. Soc.*, **132**, 1066 (2010).
12. A. D. Becke, *J. Chem. Phys.*, **98**, 5648 (1993).
13. C. Lee, W. Yang, and R. G. Parr, *Phys. Rev. B*, **37**, 785 (1988).
14. M. M. Francl, W. J. Petro, W. J. Hehre, J. S. Binkley, M. S. Gordon, D. J. DeFrees, and J. A. Pople, *J. Chem. Phys.*, **77**, 3654 (1982).
15. S. Miertuš, E. Scrocco, and J. Tomasi, *Chem. Phys.*, **55**, 117 (1981).
16. S. I. Gorelsky, *SWizard program*, University of Ottawa, Ottawa (2010). http://www.sg-chem.net.
17. Z. Chen, C. S. Wannere, C. Corminboeuf, R. Puchta, and P. v. R. Schleyer, *Chem. Rev.*, **105**, 3842 (2005).
18. P. v. R. Schleyer, C. Maerker, A. Dransfeld, H. Jiao, and N. J. R. v. E. Hommes, *J. Am. Chem. Soc.*, **118**, 6317 (1996).
19. K. Wolinski, J. F. Hinton, and P. Pulay, *J. Am. Chem. Soc.*, **112**, 8251 (1990).
20. R. Krishnan, J. S. Binkley, R. Seeger, and J. A. Pople, *J. Chem. Phys.*, **72**, 650 (1980).
21. T. Clark, J. Chandrasekhar, G. W. Spitznagel, and P. v. R. Schleyer, *J. Comp. Chem.*, **4**, 294 (1983).
22. R. W. F. Bader, *Atoms in Molecules. A Quantum Theory*, Oxford University Press, Oxford (1990).
23. T. A. Keith, *AIMAll*, *Version 10.07.25*, 2010; http://aim.tkgristmill.com.
24. M. J. Frisch, G. W. Trucks, H. B. Schlegel, G. E. Scuseria, M. A. Robb, J. R. Cheeseman, G. Scalmani, V. Barone, B. Mennucci, G. A. Petersson, H. Nakatsuji, M. Caricato, X. Li, H. P. Hratchian, A. F. Izmaylov, J. Bloino, G. Zheng, J. L. Sonnenberg, M. Hada, M. Ehara, K. Toyota, R. Fukuda, J. Hasegawa, M. Ishida, T. Nakajima, Y. Honda, O. Kitao, H. Nakai, T. Vreven, J. A. Montgomery, Jr., J. E. Peralta, F. Ogliaro, M. Bearpark, J. J. Heyd, E. Brothers, K. N. Kudin, V. N. Staroverov, R. Kobayashi, J. Normand, K. Raghavachari, A. Rendell, J. C. Burant, S. S. Iyengar, J. Tomasi, M. Cossi, N. Rega, J. M. Millam, M. Klene, J. E. Knox, J. B. Cross, V. Bakken, C. Adamo, J. Jaramillo, R. Gomperts, R. E. Stratmann, O. Yazyev, A. J. Austin, R. Cammi, C. Pomelli, J. W. Ochterski, R. L. Martin, K. Morokuma, V. G. Zakrzewski, G. A. Voth, P. Salvador, J. J. Dannenberg, S. Dapprich, A. D. Daniels, Ö. Farkas, J. B. Foresman, J. V. Ortiz, J. Cioslowski, and D. J. Fox, *Gaussian 09*, *Revision A.02*, Gaussian Inc., Wallingford (2009).
25. P. B. Karadakov, *J. Phys. Chem. A*, **112**, 12707 (2008).
26. S. J. Thompson, F. L. Emmert 3rd, and L. V. Slipchenko, *J. Phys. Chem. A.*, **116**, 3194 (2012).

27. C. B. Nielsen, T. Brock-Nannestad, P. Hammershøj, T. K. Reenberg, M. Schau-Magnussen, D. Trpcevski, T. Hensel, R. Salcedo, G. V. Baryshnikov, B. F. Minaev, and M. Pittelkow, *Chem.-Eur. J.*, **19**, 3898 (2013).
28. T. Hensel, D. Trpcevski, C. Lind, R. Grosjean, P. Hammershøj, C. B. Nielsen, T. Brock-Nannestad, B. E. Nielsen, M. Schau-Magnussen, B. Minaev, G. V. Baryshnikov, and M. Pittelkow, *Chem.–Eur. J.*, **19**, 17097 (2013).
29. G. V. Baryshnikov, B. F. Minaev, M. Pittelkow, C. B. Nielsen, and R. Salcedo, *J. Mol. Model.*, **19**, 847 (2013).
30. G. V. Baryshnikov, B. F. Minaev, N. N. Karaush, and V. A. Minaeva, *Phys. Chem. Chem. Phys.*, **16**, 6555 (2014).
31. K. Y. Chernichenko, V. V. Sumerin, R. V. Shpanchenko, E. S. Balenkova, and V. G. Nenajdenko, *Angew. Chem.*, *Int. Ed.*, **45**, 7367 (2006).
32. A. Dadvand, F. Cicoira, K. Yu. Chernichenko, E. S. Balenkova, R. M. Osuna, F. Rosei, V. G. Nenajdenko, and D. F. Perepichka, *Chem. Commun.*, 5354 (2008).
33. T. Fujimoto, M. M. Matsushita, H. Yoshikawa, and K. Awaga, *J. Am. Chem. Soc.*, **130**, 15790 (2008).
34. N. N. Karaush, B. F. Minaev, G. V. Baryshnikov, and V. A. Minaeva, *Opt. Spectrosc.*, **116**, 33 (2014).
35. C. F. Wilcox, Jr., J. P. Uetrecht, G. D. Grantham, and K. G. Grohmann, *J. Am. Chem. Soc.*, **97**, 1914 (1975).
36. T. Nishinaga, T. Ohmae, and M. Iyoda, *Symmetry*, **2**, 76 (2010).
37. S. Radenković, I. Gutman, and P. Bultinck, *J. Phys. Chem. A.*, **116**, 9421 (2012).
38. A. Yu. Sokolov, D. Brandon Magers, J. I. Wu, W. D. Allen, P. v. R. Schleyer, and H. F. Schaefer III, *J. Chem. Theory Comput.*, **9**, 4436 (2013).
39. H. Fliegl, S. Taubert, O. Lehtonen, and D. Sundholm, *Phys. Chem. Chem. Phys.*, **13**, 20500 (2011).
40. R. R. Valiev and V. N. Cherepanov, *Int. J. Quant. Chem.*, **113**, 2563 (2013).
41. R. R. Valiev, H. Fliegl, and D. Sundholm, *J. Phys. Chem. A*, **117**, 9062 (2013).
42. O. Loboda, I. Tunell, B. Minaev, and H. Agren, *Chem. Phys.*, **312**, 299 (2005).